Research Journal of Physical Sciences _____ ISSN 2320–4796
Vol. **6(1),** 1-8, January **(2018)** *Res. J. Physical Sci.*

Potassium doping effect on tungsten bronze $KxWO_3$ structure

Alain Second Dzabana Honguelet[1,2,] and Timothée NSONGO[1,2,3]*
[1]Research Group of Physical Chemical and Mineralogical Properties of Materials, Brazzaville, Congo
[2]Faculty of Science and Technology (University Marien Ngouabi), Brazzaville, Congo
[3]Center of Geological and Mining Research, Brazzaville, Congo
nsongo@yahoo.com

Available online at: www.isca.in, www.isca.me
Received 3rd November 2017, revised 30th December 2017, accepted 3rd January 2018

Abstract

The effect of potassium doping in cubic, hexagonal and monoclinical tungsten bronze $KxWO_3$ structure has been studied experimentally and by the EAM method. For the experimental method WO_3 was deposited in phase vapor deposition using reactive sputtering triode D.C method on the mica substrate. Embedded Atom Method (EAM) was used to discuss experimental results and to predict the effect of potassium content on nanorods crystallographic structure. The experimental results shows the nanorods obtained in the range of 350^0C to 550^0C with different size were observed at two directions in the potassium concentration zone. EAM analysis showed that potassium content has a significant effect both on the stability and crystallographic of nanorods structure. These results were found to be in agreement with other authors.

Keywords: Nanorods, E.A.M., embedded atom method, WO_3, tri oxide de tungsten, mica, structure.

Introduction

The study of the interior pollution of the houses has a great interest and can help to understand the origin of various unknown diseases. One of the current practices in Congo is in using oils of the engines of vehicles like protective coatings on the wood of the frames against the termites attack[1]. Chromatographic studies[2] initiated in our laboratory showed that oils of the engines contain dangerous pollutants which affect the human health.

In order to preserve the human health and to limit the impacts of these pollutants in the environment, we carried the efforts on the improvement of the quality of the oils engine, the optimization of the processes of combustion[3]. These measurements were found to be insufficient with the evolution of the produce of gas in their quality. This limitation pushed us to turn to new technologies based on the nanorods research[4].

The progress made in the field of nanorods technologies has particularly favoured the development and the evolution of the sensors physical properties and chemical such as: sensitivity, their stabilities in different range of temperature[5].

Several sensors (chemical sensors) were worked out for the gases detection application[6].

It was shown that structured nano oxides (nano rods) present physical properties more remarkable related to their size than their initial materials[7]. The study of the nano rods of WO_3 has a great interest for making of many materials in various fields such as the sensors.

Materials and methods

Substrat preparation: In order to study the structure, nanorods of WO_3, were deposited on the surface of mica using reactive sputtering triode DC methods[8].

The mica muscovite of formula KAl_2 ($AlSi_3O_{10}$) (OH, F) used as substrate has a monoclinical structure with base centered whose cell parameters measured X ray diffraction are: a=0,518 nm; b=0,899 nm; c=2,009 nm and b=95,110[9].

The experimental devices is mainly composed of a pump vacuum system with a limit vacuum pressure of the order of $1.5.10^{-5}$ Pa. The vacuum chamber is cylindrical in shape with a diameter of approximately 0.30 m and a height of 0.20 m.

Calculation procedure: We have used the EAM defined in the reference[10-13]. The EAM is a technique for construction of many body potentials models for metals developed recently by Daw and Baskes[14,15]. The total energy of the system of atoms, E_{tot} in EAM is given by:

$$E_{tot} = \sum_t E_t \quad (1)$$

$$E_{tot} = \sum_i (F_i(\rho_i) + \frac{1}{2}\sum_{j\neq i} \phi_{ij}(r_{ij})) \quad (2)$$

$$\rho_t = \sum_{j\neq i} f_j(r_{ij}) \quad (3)$$

Where the sums are over the atoms *i* and j. The subscripts *(i, j)* denote either an atom at a particular site or the type of that atom. The embedding function F_i is the energy needed to embed an atom into the background electron density at site *i*. ρ_i is the total

electron density at site *i* due to all the atoms in the system except the embed one. ϕ_{ij} is a pair interaction between atoms *i,j* whose separation is given by r_{ij}. The total energy is the total internal energy of an assembly of atoms. f_j (r_{ij}) is the contribution to the electron density at site *i* due to atom *j* at the distance r_{ij} from atom i.

Results and discussion

Experimental results: The WO_3 nanorods were prepared in the vapor phase deposition. The WO_3 was first deposited on an SiO_2 substrate and then vaporized on a mica substrate.

The growth of WO_3 nanorods with temperature can be described by growth mechanism reported by Gillet et al[8].

Nanorods of WO_3 are obtained at source-substrate distance varying in the range of 1 mm to 4 mm for temperatures ranging from 350^0C to 500^0C.

Figure-1 and 2 presents the Atomic Force Microscope selected images at two temperature. At 500^0C, the nanorods population is weak than at 350^0C.

The results show that the nanorods of WO_3 grow in two different directions. These nanorods do not cover the all surface of the mica. This observations are in agreement with recent studies[8] which have shown that the nanorods of WO_3 grow in epitaxy in predefined directions on mica substrate. The growth mechanism of the nanorods of WO_3 according to these authors can be related with the presence of potassium content[9].

Figure-1: AFM micrograph of nanorods at 350^0C.

Figure-2: AFM micrograph of nanorods at 550^0C.

EAM analysis of the influence of potassium dopage on nanorods structure compounds: bronzes of tri tungsten oxide: For the hexagonal system, the EAM results of the influence of potassium content are presented in the Table-1.

Table-1: Lattice parameters of $KxWO_3$.

Composition	a	b	c
$K_{0.27}WO_3$	7.40	7.56	/
$K_{0.31}WO_3$	7.37	7.54	/
$K_{0.26}WO_3$	7.38	7.53	/
$K_{0.33}WO_3$	7.38		3.77

However the use of bronze is function of the preferential sites for WO_3 system. A maximum rate of filling is defined for each phase of the WO_3. We present in the Table-2, the maximum occupancy rate related to the structure.

Table-2: Occupation rate as function of lattice structure.

Structure	Rate of maximum occupation
Cubic	1
Monoclinical	8
Hexagonal	1
Hexagonal II	2

Embedded Atom Method approch: The $KxWO_3$ compound can be written as a combination of potassium and tri tungsten oxide such as:

A+B=AB, avec A=K et B=WO_3

We used the approximation of the virtual crystal (VCA)[16] to calculate all the mixed physical parameters in formalism EAM. The mixed potential can be written at stoichiometric concentration in the following form:

$$\phi^{kxwo3}(r) = x\phi^{k}(r)+(1-x)\phi^{wo3}(r) \quad (4)$$

We introduce a concentration to control the potassium rate in a given structure (monoclinical, cubic, hexagonal), the potential can then be defined again such as:

$$2 * \phi^{kxwo3}(r) = \frac{y}{z}\phi^{k}(r)+ \phi^{wo3}(r) \quad (5)$$

Where: y represent the quantity of potassium and Z is the number of sites in an unspecified structure (Z=*8* for monoclinical structure defined by KxW_2O_6, Z=12 for the hexagonal structure defined by $K_xW_4O_{36}$).

The potential of the potassium used in this calculation is the potential of Morse. Potassium is element of the periodic table classified in the family of the alkaline ones. Its crystallographic form cubic is centered, therefore two atoms by primitive cell with lattice constant about 5.32 $\dot{A}$.

Table-3: Energy parameters du potassium[16].

F_{0ev}	$E_{C\,ev}$	$E_{1f\,ev}$	f_e
0.536168	0.934	0.35	0.0547

Table-4: Energies de surface[17].

Surfaces	100	110	111
Energies mjm^{-2}	139	142	148
Densités	0.438	0.218858	0.383001

Table-5: Elastic constants[17].

C11	C12	C44
0.028 ev/A°3	0.023 ev/A°3	0.016 ev/A°3

EAM potential of potassium[18].

$$\phi^k(r) = D[e^{-\alpha(r-ro)} - 2e^{-\alpha(r-ro)}] \quad (6)$$

Table-6: EAM Physical constant and parameters.

D 10^{-13} erg	r_o A°	α A^{o-1}	R_{cut} A°	βm
0.8530	0.4766	6.4130	6.5550	3.3232

We chose electronic density given for hydrogenite[19]:

$$\rho_m(r) = f_e\{r^6(e^{-\beta r} + 2^9 e^{-2\beta r})\} \quad (7)$$

With

$$f_e = \frac{(E_c - E_{1f})^{3/5}}{\Omega} \quad (8)$$

Table-7: Fitting parameters of electron density.

f_e	β	Ω
0.0547	5	$a^3/2$

The embedding energy of potassium is deduced from the complementarity of total energy

$$F(\rho) = -F_0\left[1 - nln\left(\frac{\rho}{\rho e}\right)\right]\left(\frac{\rho}{\rho e}\right)^n \quad (9)$$

With n=0,155

Potassium has an occupancy rate defined in each structure. For monoclinical structures, the maximum occupancy rate is of 8, corresponding to the number of sites has to occupy.

The number of configurations is corresponding to a particular site of potassium in the monoclinical structure of WO_3.

We set x = y/8

with y the potassium concentation by site.

Table-8: Configuration with potassium rate.

Y	Configuration
1	8
2	28
3	56
4	70

The mixed potential can be written as function of potassium occupation rate:

$KxWO_3$=x K + WO_3

Taken in account the structure ², this relation can be given in the following form:

$KxWO_3$=y/8 K + WO_3 ou Ky/8WO3=y/8 K + WO_3

Table-9: Configuration energy of cubic structure.

y	Number of configurations	Configuration Energy (y=1)
1	1	0
2	3	-0,415
3	56	-0,807
4	70	-1,219

Influence of potassium content: We fixed the values of the parameters of mixed potential according to the occupancy rate on the basis of the monoclinical systems. The Table-10 gives the various structures according to the potassium rate.

Table-10: Lattice structure as function of filling rate.

Y	a	b	c	Structure
0	7.63	7.73	7.75	Monoclinique
1	7.63	7.62	7.97	Tetragonal
2	7.70	7.71	7.83	Tetragonal
3	7.77	7.77	7.77	Cubique
4	7.80	7.80	7.80	cubique

To apprehend the part which potassium plays we used the data of the structure tetragonal of which the quantity of insertion per rate of filling is of 2 as for the cube which is of 3.

Cubic and monoclinic structure: In this section, we present the energy of the tungsten bronze after insertion of potassium to fixe the WO_3 and variable for potassium; this energy is defined by the following relation:

$$E = \frac{y}{x}E_k + E^i_{wo3} \quad (10)$$

With i=1,2 (1 – cubic, 2-hexagonal)

Cubic system: E.A.M simulation of the tungsten bronze of formula cubic $KxWO_3$ phase was made and we observed modifications the energy of the system, the density, the embedding energy and mixed potential for values of the potassium x concentration ranging between 0.125 and 0.875.

We showed that for values of x ranging between 0.125 and 0.875, the $Vx_{-1}<Vx$ potential and energy $Ex_{-1}> Ex$ as for the density $\rho x_{-1}>\rho x$. Finally for the EAM embedding function, $Fx_{-1}> Fx$, we obtain the effect of the concentration on the cell parameter.

Embedding Energy: We represent the energy of insertion for various values of the concentration of potassium.

For values of x higher than 0.5, the embedding energy presents different minima.

A variation is observed for x between 0,3 and 0,4 that we named interval of stability, for x between 0,5 and 0,6 the system becomes increasingly stable that precedents.

Electronic density of $KxWO_3$: The electronic density is most important in formalism EAM, we calculated the numerical values of the density at the point of balance given by energy of insertion. The Figure-2 gives the results.

We notice that these densities are found to be different for values of x ranging between 1 and 1,85 become identical for the x higher than 1,85 whatever the concentration.

Mixed potential: The interaction between potassium and grouping WO_3 is represented in the Figure-3, it reveals that more the concentration increases more the minimum values increases. The change of this minimum values must relate the stability of the system to the potassium concentration.

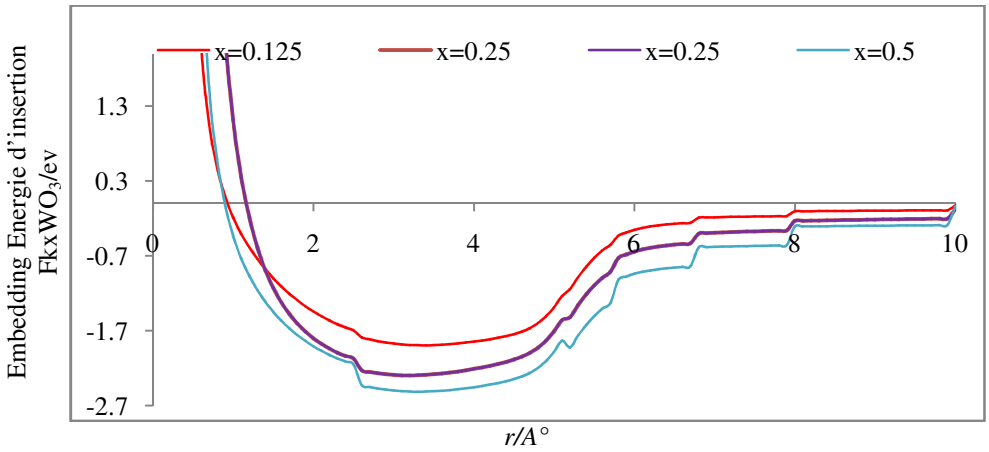

Figure-1: Embedding energy for F $KxWO_3$ with cubic structure.

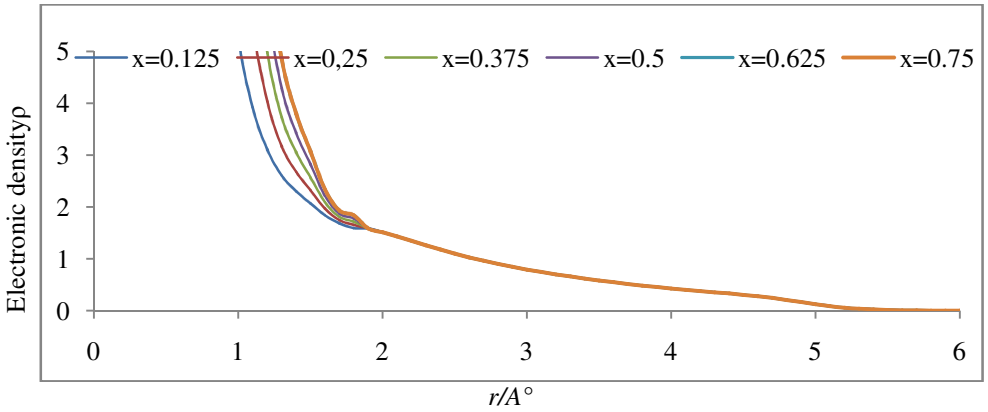

Figure-2: $KxWO_3$ electronic density as function of potassium concentration.

Energy of the system: We calculated the energy of the system, the results obtained are presented on the Figure-4.

For the cubic system of the WO_3, the maximum energy is given by the following formula:

$$E^{i}_{wo3} = 0.25 * E_{w\_bcc} + 0.75 * E_O \quad (11)$$

The energy system presents a minimum at the same value. No shift of the values Re is observed, it means the potassium concentration has no effect on the system stability.

Hexagonal structure: The hexagonal system is metastable for system WO_3, however it presents important sites in the face to be able to receive the alkaline in order to form bronze.

From the energy point of view, we showed that the energy of the system $KxWO_3$ depends enormously on the structure of W (hcp or BCC), the knowledge of various energies of the crystallographic structures of W will lead to predict the average energy of the $KxWO_3$.

We notice that the densities are considerably different for values of x ranging between 1 and 1,85 beyond whose the values all become identical.

We located then the values of R to balance and deduced the values from the corresponding densities. We observe a maximum of filling for values of x between 0,25 and 0,35 and a saturation for values of x between 0,5 and 0,8.

The interaction between potassium and WO_3 is presented in the Figure-5, it reveals well that more the concentration increases, the minimum decreases when system is stabilized.

We calculated the energy of the system, which enabled us to plot the curves according to the concentration of potassium (Figure-6).

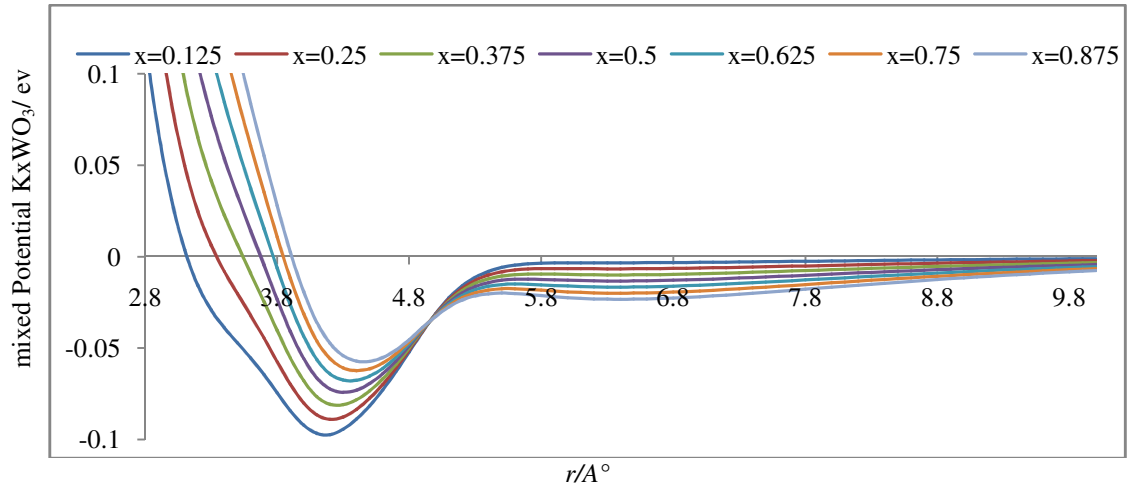

Figure-3: Mixed potential of $KxWO_3$ as function of potassium concentration.

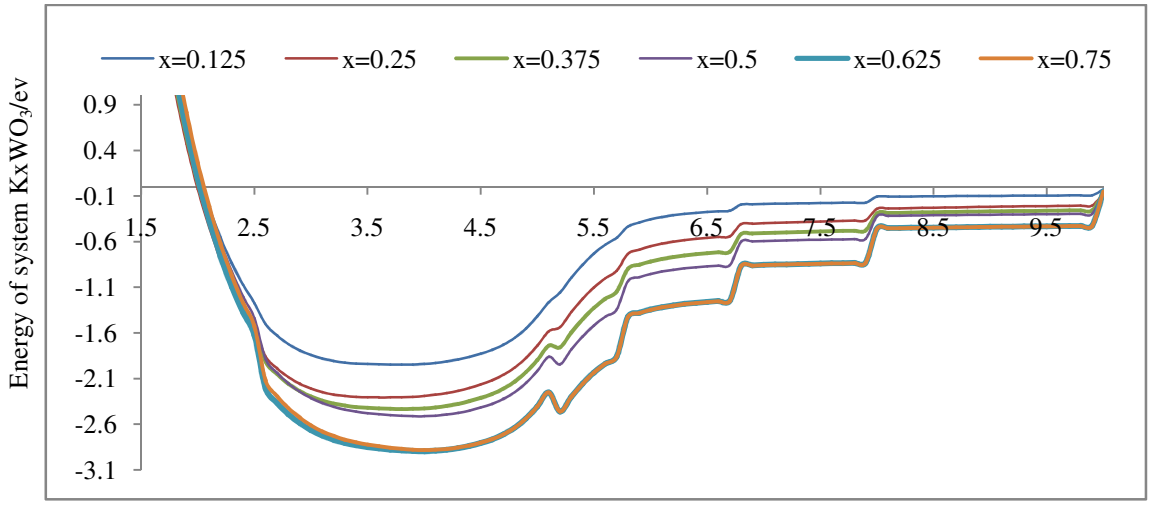

Figure-4: Energy of $KxWO_3$ as function of potassium concentration.

We notice a shift of the values Re related to the potassium concentration. For the cubic system of the WO_3 we have

$$E^{i}_{wo3} = 0.25 * E_{w}\_hcp + 0.75 * E_{O} \quad (13)$$

Monoclinical structure: We made for the monoclinical system a study which takes into account the distortions and the effect of potassium for the cell parameters.

We however studied this system in the theory of the transitions to see the effect of potassium on the cell parameters.

For the hexagonal system, a study will take into account the distortions and also we took into account the effect of potassium for the cell parameters.

The energy of the $KxWO_3$ system doesn't not depend enormously on the crystallographic structure of W (hcp or BCC), it will not be enough to know various energies of the crystallographic structures of W to predict the average energy of the $KxWO_3$.

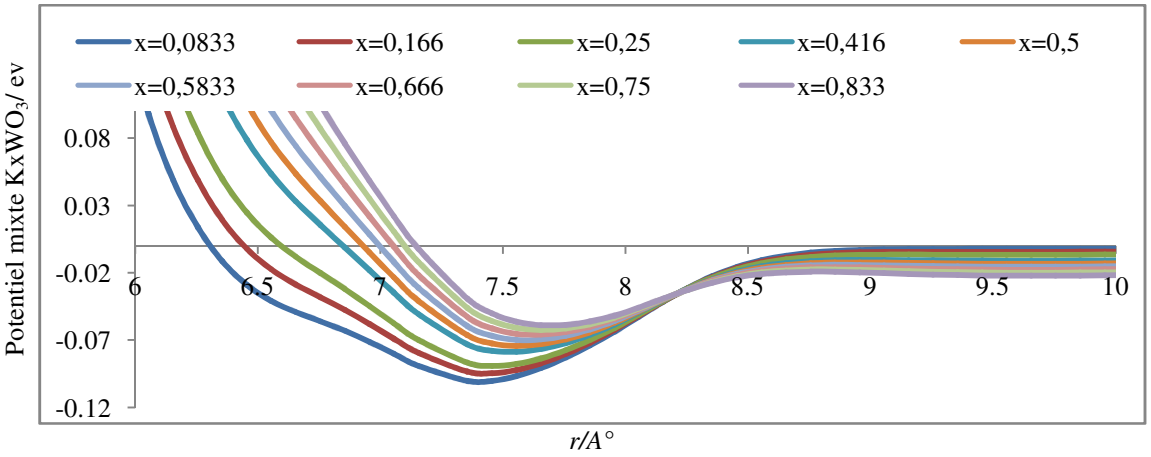

Figure-5: Mixed potential for $KxWO_3$ as function of potassium concentration.

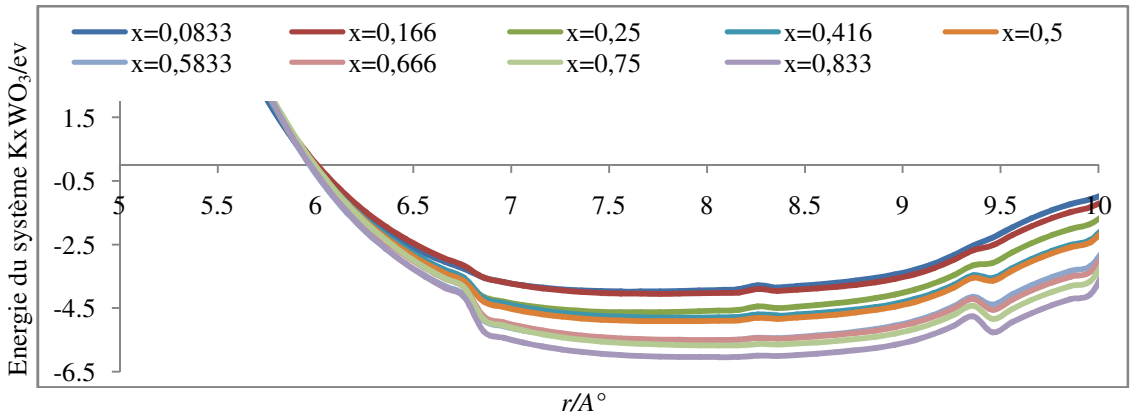

Figure-6: Energy of $KxWO_3$ en fonction de la concentration du potassium.

Table-11: Physical parameter as function of potassium content for cubic and hexagonal structure of $KxWO_3$.

	E		Potential		Embedding function F(ρ)	
Potassium concentrationx	Cubic structure	Hcp structure	Cubic structure	Hcp structure	Cubique structure	Hcp structure
0.1	-3,8940044	-4,048561	-19,46	-18,92	-3,7873768	-4,021356
0.2	-4,60761208	-4,726324	-17,8	-17,8	-4,598669	-4,637324
0.375	-4,86488574	-4,771638	-16,18	-15,74	-4,8798562	-4,614238
0.4	-5,02441688	-4,903226	-14,84	-15,74	-5,0329008	-4,824526

Table-12: EAM functions for cubic and hexagonal $KxWO_3$ structure.

x_k	0.1-375			0.375-0.4		
	Energy	Embedding energy	Potential	Energy	Embedding energy	potential
1^e	Hexagonal	hexagonal	cubique	cubique	cubique	cubique
2^e	Cubique	cubique	cubique	cubique	cubique	hexagonal

For the monoclinic system, we carried out a study that takes into account distortions and the effect of potassium on mesh parameters. We have, however, studied this system in the theory of transitions to see the effect of potassium on mesh parameters.

We have realized for the hexagonal system a study will take into account the distortions and also we took into account the effect of the potassium for the parameters of mesh. From the energy point of view, we have shown that the energy of the $KxWO_3$ system depends enormously on the crystallographic structure of the W (hcp or bcc), it will be sufficient to know the different energies of the crystallographic structures of w to predict the average energy of $KxWO_3$.

Conclusion

The experimental method based on sputtering reactive triode D.C. was used to obtain nanorods on mica surface. The AFM observations showed that nanorods of different size of WO_3 can be located on the mica surface in the zone with potassium concentration. Theses nanorods growed in two different directions at the temperature ranging between 350°C to 550°C. The E.A.M model was used to discuss the influence of the potassium concentration on nanorods structure. It was find that the potassium content has a strong effect on the stability and the structure of $KxWO_3$.

References

1. Alban Mouanda Moussitou, Etude chromatographique en phase gazeuse des huiles appliquées sur les charpentes en bois à l'intérieur des habitations). Master dissertation, Université Marien Ngouabi, 2017

2. Timothée Nsongo, Hilaire Elenga, Bernard Mabiala, David Bilembi and Ferland Ngoro (2016). ELENGA, study of the pollution generated by engine oils applied on building woods to control termites. *International Journal of Research in Environmental Science,* 2(6), 12-18.

3. Pinter Z. (2002). Caractérisation de couches épaisses de semi-conducteur WO_3 et WO_3/TiO_2 pour la réalisation de capteurs à NO2 (Doctoral dissertation, Lyon, INSA).

4. Bruyere S. (2010). Structure et croissance de nanophases supportées d'oxyde de tungstène (Doctoral dissertation, Université de Bourgogne).

5. Balázsi C., Wang L., Zayim E.O., Szilágyi I.M., Sedlacková K., Pfeifer J. and Gouma P.I. (2008). Nanosize hexagonal tungsten oxide for gas sensing applications. *Journal of the European Ceramic Society*, 28(5), 913-917.

6. Institut national de recherche et de sécurité (INRS*), détecteurs portables de gaz et de vapeurs ; guide de bonnes pratiques pour le choix, l'utilisation et la vérification*, février 2011 ;

7. Dipero L.E, Ferroni M., Guidi V, Marca G., Martenelli G., Nelli P., Sangaletti L. and Sberveglieri G. (1996). preparation and microstructure charactérisation of nanosized thin film of TiO_2-WO_3 as a novel material with hight sensibility towards NO_2. *sensors and actuators B* ; *chemical*, 36, 381-383.

8. Gillet M., Delamare R. and Gillet E. (2005). Growth of epitaxial tungsten oxide nanorods. *journal of Crystal Growth*, 279, 93-99.

9. Gillet M., Delamare R. and Gillet E. (2005). Growth, structure and electrical properties of tungsten oxide nanorods. *The European Physical Journal D-Atomic, Molecular, Optical and Plasma Physics*, 34(1), 291-294.

10. Daw M.S. and Baskes M.I. (1984). Molecular dynamic simulation of glass formation in binary liquid metal: Cu–Ag using EAM. *Phys.Rev.B,* 29, 6443.

11. Rose J.H., Smith J.R., Guinea F. and Ferrante J. (1984). Universal features of the equation of state of metals. *Physical Review B*, 29(6), 2963.

12. Finnis M.W. and Rühle M. (1993). Structures of interfaces in crystalline solids. *Materials Science and Technology*, 1, 533.

13. Gupta R.P. (1981). Lattice relaxation at a metal surface. *Physical Review B*, 23(12), 6265.

14. Hohenberg H. and Kohn W. (1964). Inhomogeneous electron gaz. *Phys.Rev.*B, 136, 864.

15. Stott M.J. and Zaremba E. (1980). Quasiatoms: An approach to atoms in nonuniform electronic systems. *Physical Review B*, 22(4), 1564.

16. Mohamed Benhamida (2014). Propriétés structurale, élastiques et électronique d'alliages de nitrure des métaux de transitions. thèse, université de setif1.

17. Akpata Erhieyowe and all (2014). Surface energy calculation of low index group 1 alkali metals of the périodic table using the modified analytical EAM. *IJRET*, Aout.

18. Xiao-Jian Y., Nan-Xian C. and Jiang S. (2012). Construction of embedded-atom-method interatomic potentials for alkaline metals (Li, Na, and K) by lattice inversion. *Chinese Physics B*, 21(5), 053401.

19. Lincoln R.C., Koliwad K.M. and Ghate P.B. (1967). Morse-potential evaluation of second-and third-order elastic constants of some cubic metals. *Physical Review*, 157(3), 463.